

1,8-Bis(tetramethylguanidino)naphthalene (TMGN): A New, Superbasic and Kinetically Active “Proton Sponge”

Volker Raab, Jennifer Kipke, Ruth M. Gschwind, and Jörg Sundermeyer*^[a]

Dedicated to Professor Rolf Gleiter on the occasion of his 65th birthday

Abstract: 1,8-Bis(tetramethylguanidino)naphthalene (TMGN, **1**) is a new, readily accessible, and stable “proton sponge” with an experimental pK_{BH^+} value of 25.1 in MeCN, which is nearly seven orders of magnitude higher in basicity than the classical proton sponge 1,8-bis(dimethylamino)-naphthalene (DMAN). Because of the sterically less crowded character of the proton-accepting sp^2 -nitrogen atoms, TMGN also has a higher kinetic basicity than DMAN,

which is shown by time-resolved proton self-exchange reactions. TMGN is more resistant to hydrolysis and is a weaker nucleophile towards the alkylating agent EtI in comparison to the commercially available guanidine 7-methyl-1,5,7-triazabicyclo[4.4.0]dec-5-ene (MTBD).

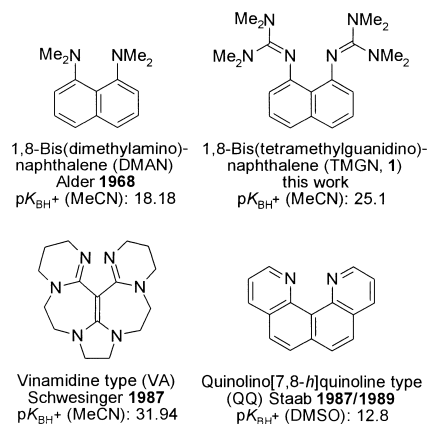
Keywords: basicity • NMR spectroscopy • peralkylated guanidines • protonation • proton sponges

Crystal structures of the free base, of the mono- and bisprotonated base were determined. The dynamic behavior of all three species in solution was investigated by variable-temperature ^1H NMR experiments. ΔG^\ddagger values obtained by spectra simulation reveal a concerted mechanism of rotation about the C–N bonds of the protonated forms of TMGN.

Introduction

For over three decades, neutral organic bases with chelating proton-acceptor functionalities have attracted particular interest. On account of their high proton affinity, they are named “proton sponges” according to the classical example 1,8-bis(dimethylamino)naphthalene (DMAN) that was introduced by Alder et al.^[1, 2] The field has been reviewed by Staab and Saupe,^[3] and more recently by Llamas-Saiz et al.,^[4] as well as in a limited manner on 1,8-diaminonaphthalene derivatives by Pozharskii.^[5] Proton sponges are still the focus of current research activity^[6] and are also the subject of vivid interest of theoretical chemists.^[7] A general feature of all proton sponges is the presence of two basic nitrogen centers in the molecule, which have an orientation that allows the uptake of *one* proton to yield a stabilized $[\text{N}\cdots\text{H}\cdots\text{N}]^+$ intramolecular hydrogen bond (IHB). Compared to ordinary alkyl and aryl amines, amidines, and guanidines, such proton chelators present a dramatic increase in basicity on account of

i) destabilization of the base as a consequence of strong repulsion of unshared electron pairs, ii) formation of an IHB in the protonated form and iii) relief from steric strain upon protonation. Two general concepts to raise the thermodynamic basicity or proton affinity have been followed. One is to replace the naphthalene skeleton by other aromatic spacers, such as fluorene,^[8] heterofluorene,^[9] phenanthrene,^[10] and biphenyl,^[11] thus influencing the basicity by varying the nonbonding $\text{N}\cdots\text{N}$ distance of the proton-acceptor pairs. The other concept focuses on the variation of the basic nitrogen centers^[6d,e, 12, 13, 14] or its adjacent environment (“but-tressing effect”).^[2, 3, 5, 15, 16]



Scheme 1. Representative “proton sponges” in relation to TMGN (**1**).

[a] Prof. Dr. J. Sundermeyer, Dr. V. Raab, Dr. J. Kipke, Dr. R. M. Gschwind
 Fachbereich Chemie, Philipps-Universität Marburg
 Hans-Meerwein-Strasse, 35032 Marburg (Germany)
 Fax: (+49)6421-28-28917
 E-mail: jsu@chemie.uni-marburg.de

Supporting information for this article is available on the WWW under <http://www.wiley-vch.de/home/chemistry/> or from the author.

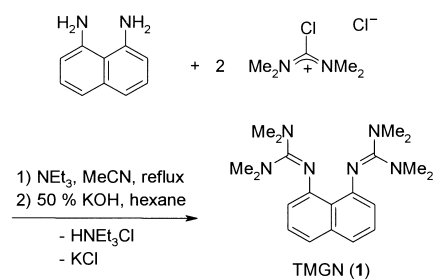
There is a trend that proton sponges with high thermodynamic basicity typically have a low kinetic basicity: The captured proton does not usually take part in rapid proton exchange reactions, which would allow such neutral superbases to serve as catalysts in salt-free base-catalyzed reactions. A successful strategy to overcome the kinetic inertness has been presented by Schwesinger et al., who developed a thermodynamically strong and at the same time kinetically active superbase that incorporates the vinamidine structure (see above).^[17] However, its multistep synthesis, moderate stability, and moderate solubility in aprotic solvents are some limitations of this proton sponge, which takes up *two* protons in the presence of excess acid.

After an examination of the reported strategies to increase the basicity of 1,8-diaminonaphthalene proton sponges and being aware that peralkyl guanidines belong to the strongest organic neutral bases known,^[18] we decided to use the tetramethylguanidino group as an efficient and straightforward modification of the chelating proton acceptor. Peralkylguanidines are several orders of magnitude higher in basicity than tertiary amines because of the excellent stabilization of the positive charge in their resonance-stabilized cations.^[19] This trend may be demonstrated by the pK_{BH^+} (MeCN) values of the 1,2,2,6,6-pentamethylpiperidinium cation (18.62), the parent guanidinium cation (23.3), and the pentamethylguanidinium cation (25.00).^[19c] It is interesting to note that pK_{BH^+} values of a wide range of nonchelating *N*-aryl guanidines have been determined^[20] and that one promising candidate for proton chelation, 2,2'-bis(tetramethylguanidyl)-1,1'-biphenyl, did not exhibit proton sponge properties, such as formation of an IHB.^[21] Dissociation constants and kinetics of proton-transfer reactions of nonchelating guanidine bases in acetonitrile^[22] as well as DMAN systems^[15a,b, 23] have been the subject of previous detailed studies.

In the present paper, we report on the synthesis as well as the spectroscopic and structural properties of 1,8-bis(tetramethylguanidino)naphthalene (TMGN (**1**), see above) and its mono- and bisprotonated forms. Surprisingly, this new proton sponge, which has a basicity that is higher by the factor of more than 10^7 than Alder's classical DMAN, was successfully prepared by a one-step synthesis in high yield. It is relatively stable towards autoxidation, soluble in aprotic nonpolar solvents and, in contrast to DMAN, it is kinetically active in proton-exchange reactions.

Results and Discussion

Synthesis: TMGN (**1**) is synthesized by a method previously described by us for the synthesis of multidentate metal-chelating oligoguanidines.^[24] Tetramethylchloroformamidinium chloride^[25] is treated with 1,8-diaminonaphthalene in the presence of triethylamine as an auxiliary base and in MeCN as the solvent. After deprotonation of the guanidinium cation with 50% aqueous KOH and extraction into hexane, **1** is obtained in analytically pure form (Scheme 2). In comparison to other proton sponges of similar basicity, this represents a rather simple synthesis from convenient precursors, as the Vilsmeier salt $[\text{ClC}(\text{NMe}_2)_2]\text{Cl}$ and related electrophiles may



Scheme 2. Synthesis of TMGN (**1**).

be produced on a large scale from ureas and phosgene or oxalyl chloride.

Reactivity studies: TMGN (**1**) is cleanly monoprotonated by an equimolar amount of NH_4PF_6 in MeCN to yield $[\mathbf{1}+\text{H}][\text{PF}_6]$ (**2a**). Colorless single crystals are obtained by slow diffusion of dry diethyl ether into the MeCN solution.

Surprisingly, monoprotonated $[\mathbf{1}+\text{H}]^+$ does not show the kinetic inertness with respect to bisprotonation, that is typical for many proton sponges. Similar to the kinetically active vinamidine proton sponge of Schwesinger,^[17] it readily takes up a second proton when treated with an excess of strong acids, such as trifluoromethanesulfonic acid, tetrafluoroboric acid etherate, trifluoroacetic acid, aqueous hexafluorophosphoric acid, or gaseous HCl. However, complete bisprotonation could not be achieved by excess NH_4PF_6 in MeCN. Colorless single crystals of $[\mathbf{1}+2\text{H}][\text{Cl}, \text{Cl}_2\text{H}]$ (**3a**) were obtained after excess hydrogen chloride was passed through a CH_2Cl_2 solution of **1** and crystallization from MeCN. Bisprotonation is a rather unusual feature observed in only a small number of proton sponges, including those of high kinetic basicity or those without a strong IHB.^[16a, 17, 26, 27] In order to distinguish between both cases, we decided to determine the crystal structures of the base and its protonated forms.

TMGN (**1**) is perfectly stable towards hydrolysis under acidic conditions (1M D_3O^+ , 25 °C, 6 d). The hydrolysis of **1** in basic media was monitored by ^1H NMR (0.83M NaOD in $[\text{D}_6]\text{DMSO}/\text{D}_2\text{O}$) and compared to the commercially available guanidine 7-methyl-1,5,7-triazabicyclo[4.4.0]dec-5-ene (MTBD). While **1** is stable at room temperature for 24 h, hydrolysis of MTBD is observed. At elevated temperatures (60 °C, 5 d), 44% of **1** and 73% of MTBD is hydrolyzed to the corresponding urea.

In order to evaluate the nucleophilicity of **1**, an alkylation reaction of **1** and MTBD with $\text{C}_2\text{H}_5\text{I}$ was performed under identical conditions (2.5 equiv $\text{C}_2\text{H}_5\text{I}$ per guanidine function, 25 °C, CD_2Cl_2). While no conversion of **1** was observed after 15 min by means of ^1H NMR, $\approx 50\%$ of MTBD was converted into the ethyl guanidinium salt. At longer reaction times (3 d, 25 °C) even less nucleophilic **1** was converted into a mixture of protonated and alkylated products, which however, could not be quantified because of signal overlap.

Structure of the base 1: Single crystals of TMGN suitable for X-ray crystallography were obtained by crystallization from hexane. The result of the structural analysis is shown in Figure 1.

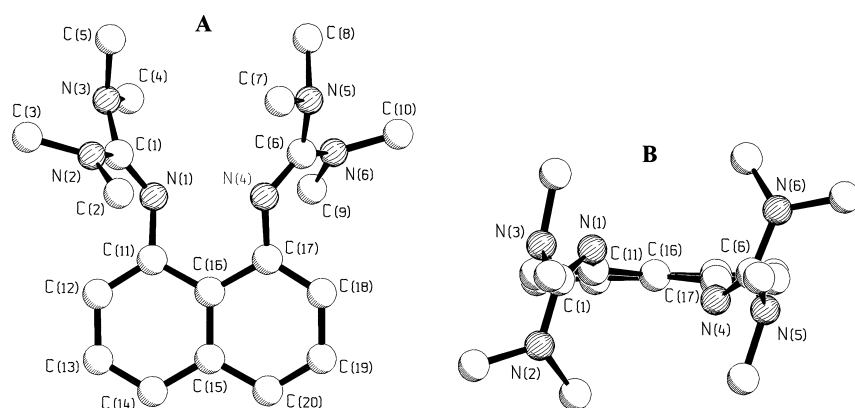


Figure 1. Molecular structure of TMGN (**1**). View perpendicular to the naphthalene ring plane (A) and projection along the C_2 axis C(16)–C(15) of the molecule (B).^[66]

Selected bond lengths and angles are given in Table 1. The molecular structure of **1** is close to C_2 symmetric with only small deviations from ideal symmetry as a consequence of the strong repulsion of the two lone pairs centered at the proton-acceptor sp^2 -nitrogen atoms N(1) and N(4) in an *anti*-orientation.

Both guanidinium centers C(1) and C(6) are trigonal planar ($\Sigma \chi = 359.9^\circ$, Table 1). As found in other peralkyl oligoguanidines,^[24a,b] the four dimethylamino groups in the periphery deviate from ideal conjugation with the C(1)N₃ and C(6)N₃ planes as indicated by torsion angles N–C–N–C of 8–45°. A similar propeller-like distortion as a result of steric repulsions has been found for the ground state of the hexamethylguanidinium cation.^[28] The guanidinium double bonds C(1/6)–N(1/4) (128.2 ± 0.1 pm) are shorter by a factor of 0.93 than the average bonding lengths of C(1) and C(6) to the peripheral NMe₂ nitrogen atoms (138.4 ± 0.1 pm).

Some characteristic structural features reveal differences in the steric constraint of TMGN and the sterically more crowded DMAN^[29] and less crowded quinolino[7,8-*h*]quinoline (QQ, see Introduction)^[14a] (corresponding values in

brackets). The indicators are the angle C(11)–C(16)–C(17) 122.6° (DMAN: 125.8°; QQ: 125.4°) of the naphthalene ring, the nonbonding distance C(11)⋯C(17) 251.9 pm (DMAN: 256.2; QQ: 258.3), and the very short nonbonding distance between the acceptor atoms N(1)⋯N(4) 271.7 pm (DMAN: 279.2; QQ: 272.7; 1,8-diaminonaphthalene: 272 pm^[51]). Additional evidence for the extent of distortion comes from the average *anti*-coplanar torsion angles within the naphthalene skeleton C(11/17)–C(16)–C(15)–C(20/14) 173.0° (DMAN: 170.3°; QQ: 178.9°) and with respect to the twisted nitrogen-donor atoms N(1/4)–C(11/17)–C(16)–C(15) 161.4° (DMAN: 168.2; QQ: 177.8). Because of the different hybridization of the N-atoms (sp^2) compared to typical proton sponges (sp^3), the *anti*-conformation of the unshared electron pairs is more easily realized, as can be seen at the position of the imine nitrogen atoms in Figure 1B. In addition, the average *syn*-coplanar torsion angle C(1/6)–N(1/4)–C(11/17)–C(12/18): 55.5° (**1**) reveals that the degree of conjugation between the π -systems of the naphthalene ring and the guanidinium moiety is marginal.

Structure of monoprotonated 1: The result of the structural analysis is shown in Figure 2; selected bond lengths and angles are given in Table 1. In [**1**+H][PF₆] (**2a**), the C_2 symmetry of the corresponding base structure is not preserved. The naphthalene system is flattened and can be considered virtually planar with the captured proton located between the imine nitrogen atoms in the same plane. There are no significant interactions between the PF₆[−] anion and the cation of **2a**.

Table 1. Selected bonding and nonbonding distances [pm], angles, dihedral angles, and bond angle sums [°] in TMGN (**1**), [**1**+H][PF₆] (**2a**), and [**1**+2H][Cl, Cl₂H] (**3a**).^[a]

	TMGN (1)	[1 +H][PF ₆] (2a)	[1 +2H][Cl, Cl ₂ H] (3a)
C(1)–N(1)	128.1(3)	135.1(6)	136.6(3)
C(6)–N(4)	128.3(3)	132.6(6)	136.5(3)
C–NMe ₂ (average)	138.4 ± 0.1	134.2 ± 2.0	133.1 ± 0.4
C(11)–N(1)	140.1(3)	140.9(6)	142.6(3)
C(17)–N(4)	139.6(3)	141.4(6)	143.4(3)
N(1)–H(1A)	–	91(6)	90(3)
N(4)–H(1A)/H(4)	–	175(6)	92(3)
N(1)⋯N(4)	271.7(3)	259.3(5)	288.1(3)
C(11)⋯C(17)	251.9(3)	255.3(7)	258.2(4)
C(11)–C(16)–C(17)	122.6(2)	124.6(4)	127.8(2)
C(11/17)–C(16)–C(15)–C(20/14)	173.7(2)/172.3(2)	178.7(4)/178.9(4)	178.2(2)/177.3(2)
N(1/4)–C(11/17)–C(16)–C(15)	–161.6(2)/–161.2(2)	177.4(1)/–171.0(4)	–172.5(2)/–174.8(2)
C(16)–C(11/17)–N(1/4)–H(1A/4A)	–/–	–9(4)/–	62.58(1)/68.66(0)
C(1/6)–N(1/4)–C(11/17)–C(12/18)	57.7(3)/53.2(4)	–10.3(8)/49.2(7)	31.4(3)/–34.1(3)
$\Sigma \chi$ N(1)	–	360.0	350.6
$\Sigma \chi$ N(4)	–	–	351.5
$\Sigma \chi$ C(1)	359.9	360.0	360.0
$\Sigma \chi$ C(6)	359.9	359.9	360.0
$\Sigma \chi$ N _{Me2} (average)	353.2 ± 3.9	359.0 ± 1.1	359.7 ± 0.3

[a] Crystallographic standard deviations in parentheses, calculated average values are given with the corresponding standard deviation (±).

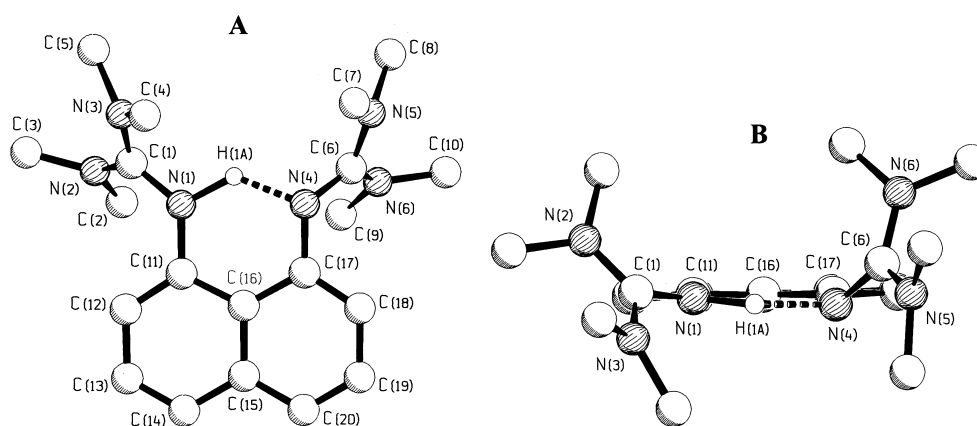


Figure 2. Molecular structure of $[1+H][PF_6]$ (**2a**). View perpendicular to mean ring plane (A) and projection along C(15)–C(16) (B), anion omitted for clarity.^[66]

In monoprotonated TMGN, the bond lengths between C(1/6) and N(1/4) become elongated, in bisprotonated species they become equivalent to the peripheral C–NR₂ bonds (Table 1). This is in agreement with the existence of a true IHB in the monoprotonated form of TMGN (further evidence is provided by the results of dynamic NMR spectroscopy, see below).

The guanidine nitrogen atoms N(1)⋯N(4) of **2a** are found at a closer distance of 259.3 pm compared with **1** (271.7 pm), which is in the range of the average value of 258 pm in DMANH⁺ structures.^[5, 30] The torsion angles for the evaluation of planarity within the naphthalene ring indicate that it is flattened to a large degree. On protonation, the angle C(11)–C(16)–C(17) is stretched to 124.6° in **2a**, while it remains essentially unchanged in DMANH⁺ 125.6°.^[30c] This trend is in agreement with an elongation of the C(11)⋯C(17) distance to 255.3 pm (DMANH⁺: 253.9). Furthermore, the average *anti*-coplanar torsion angles C(11/17)–C(16)–C(15)–C(20/14) 178.8° (DMANH⁺: 178.7) and the twisting of the donor atoms N(1)–C(11)–C(16)–C(15) and N(4)–C(17)–C(16)–C(15) are 177.4° and 171.0°, respectively, (DMANH⁺: 179.6° and 177.7°) and indicate the trend of planarization. The proton was found and isotropically refined. For confirmation of the exact position of the proton or differentiation of the imine nitrogen atoms, a neutron diffraction structure analysis^[31] and ESCA spectroscopy,^[32] respectively, would be the method of choice. The proton is localized unsymmetrically in a nonlinear hydrogen bridge N(1)–H(1A)⋯N(4), as indicated by the short N(1)–H(1A) bond length of 91 pm, a long distance N(4)⋯H(1A) of 175 pm, and an N(1)–H(1A)⋯N(4) angle of 152°. A similar geometry has been found in other proton sponges (Table 2).

The *syn*-coplanar torsion angles, which indicate the probability of p-orbital overlap C(1/6)–N(1/4)–C(11/17)–C(12/18), differ significantly for both guanidine groups of **2a**. While the guanidine group with the smaller N–H bond length has a torsion angle of only 10.3°, which permits conjugation, the other group displays a torsion angle of almost 50°, similar to **1**.

Structure of bisprotonated 1: The X-ray structure of $[1+2H][Cl, Cl_2H]$ (**3a**) is shown in Figure 3; selected bond lengths and angles are given in Table 1, the hydrogen atoms

Table 2. Comparison of N–H bond lengths [pm] and angles [°] in various proton sponges with $[1+H][PF_6]$ (**2a**) and $[1+2H][Cl, Cl_2H]$ (**3a**).

Compound	N⋯N	N–H	H⋯N	N–H⋯N
[DMANH]CIMH ^[a]	264.4(2)	110.6(5)	160.8(6)	153.3(5)
[DMANH]HS ^[b]	258.3(2)	108(2)	155(2)	157(2)
[TDMANH ₂]Br ₂ ^[c]	256.7(5)	122(1)	139(1)	158
[VAH](BPh ₄) ^[d]	254.1	92.0(3)	178(1)	137.6
[VAH ₂](ClO ₄) ₂ ^[d]	284.5	86.0(34)/86.0(49)	–	–
$[1+H][PF_6]$ (2a)	259.3(5)	91(6)	175(6)	152(5)
$[1+2H][Cl, Cl_2H]$ (3a)	288.1(3)	90(3)/92(3)	–	–

[a] 1-Dimethylamino-8-dimethylammonionaphthalene 1,2-dichloromaleate, determined by means of neutron diffraction.^[31] [b] 1-Dimethylamino-8-dimethylammonionaphthalene hydrogen squarate.^[30c] [c] 5,8-Bis(dimethylamino)-1,4-bis(dimethylammonio)naphthalene dibromide.^[39] [d] Vinamidine.^[17]

H(1), H(4), and H(2) were found and isotropically refined. In the dication **3a**, the planarity of the naphthalene ring observed in **2a** is essentially maintained while the guanidinium units are increasingly twisted with respect to each other. The protons adopt a *syn*-conformation with hydrogen bonding to a bridging chloride anion so that the inner core of the molecule has almost C_s symmetry. The chelating hydrogen bond lengths are 221(3) pm for N(1)–H(1)⋯Cl(1) and 229(3) pm for N(4)–H(4)⋯Cl(1). A solvate with hydrogen chloride is formed by a second chloride anion. The resulting anion $[Cl-H⋯Cl]^-$ reveals an unsymmetrical linear hydrogen bond similar to the structurally characterized example $[H_3O \cdot 18\text{-crown-6}][Cl_2H]^{[33]}$ within a variety of characteristic bond lengths and angles that have been found for this anion (Table 3).

As a result of the second protonation, the angle C(11)–C(16)–C(17) is further enlarged to 127.8°, the nonbonding distances C(11)⋯C(17) 258.2 pm and N(1)⋯N(4) 288.1 pm

Table 3. Comparison of Cl–H⋯Cl bond lengths [pm] and angles [°] in $[1+2H][Cl, Cl_2H]$ (**3a**) with structurally characterized reference compounds containing the $[Cl_2H]^-$ anion.

Compound	Cl–H	Cl⋯H	Cl–H⋯Cl
$[1+2H][Cl, Cl_2H]$ (3a)	145(5)	170(5)	177(2)
[AsPh ₄][Cl ₂ H] ^[60]	154.6	154.6	180.0
$[H_3O \cdot 18\text{-crown-6}][Cl_2H]^{[33]}$	147.1	164.9	168.2
[(Me ₃ NH) ₂ Cl][Cl ₂ H] ^[61]	138.4	178.6	163.2

are also elongated. These parameters reflect a dramatic increase in steric strain as a result of bisprotonation: Both protons point towards the bridging chloride ion, the guanidine functions adopt a *syn*- and not an *anti*-conformation. As a result, the guanidine N-atoms lie almost in the same plane as the naphthalene ring, as indicated by the *anti*-coplanar torsion angles N(1/4)-C(11/17)-C(16)-C(15) 172.5 and 174.8°. This sterically congested conformation is stabilized through hydrogen bonds to the chloride anion (Figure 3).

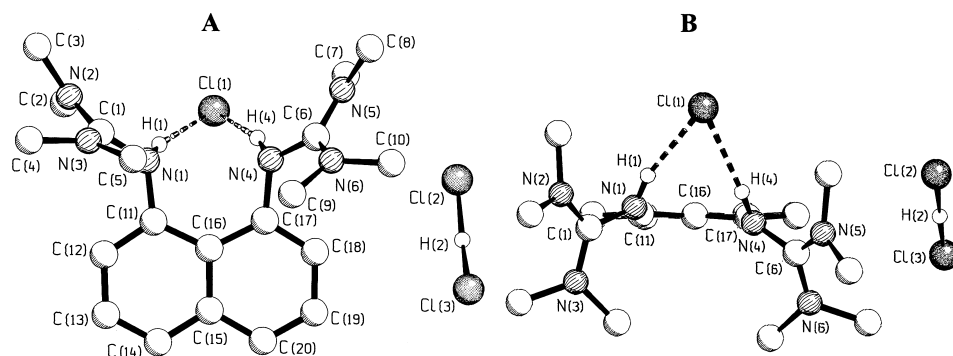


Figure 3. Molecular structure of [1+2H][Cl, Cl₂H] (**3a**). View perpendicular to mean ring plane (A) and front view along C(15)–C(16) (B).^[66]

The planarity of the naphthalene ring is expressed by its average *anti*-coplanar torsion angle C(11/17)-C(16)-C(15)-C(20/14) 177.8°. In **3a**, the *syn*-coplanar torsion angles (C(1/6)-N(1/4)-C(11/17)-C(12/18)) relevant to evaluate a conjugation are approximately 33°.

The reaction of **1** with aqueous hexafluorophosphoric acid gave light brown crystals, which were subjected to an X-ray analysis that identified the product as [1+2H][PF₆, BF₄] (**3b**). This surprising result arises from an HBF₄ impurity in the HPF₆ introduced in the manufacturing process, as has been previously reported.^[34] Further evidence for the BF₄⁻ anion is provided by NMR (¹⁹F, ³¹P, ¹¹B) as well as ESI mass spectrometry (see the Experimental Section). Even though the *R* values of its structure resolution were rather poor because of twinning and disorder of the anions, the proportions in the naphthalene cation can be considered accurate according to the temperature factors of cation versus anion. Without going into a detailed discussion of structural parameters, one specific difference between **3a** and **3b** should be pointed out: While the two protons are in a *syn*-conformation in **3a**, in **3b** an *anti*-conformation is realized with essentially non-coordinating anions. Thus, the energetic difference between the *syn*- and *anti*-conformers cannot be very high. This is also documented by the small difference in the populations revealed by dynamic NMR studies of solutions of bisprotonated **3c** (see below).

NMR spectra and pK_{BH+}: The 400 MHz ¹H NMR spectrum of [1+H][PF₆] (**2a**) in CD₃CN shows a broad signal at δ = 14.28 for the NH proton. This relatively moderate downfield shift of the NH proton in **2a** compared to δ ≈ 18.6 (CD₃CN) in DMAN and other naphthalene-based proton sponges,^[5] or even δ = 19.38 ([D₆]DMSO) for QQ, is assigned to the formation of a weaker, unsymmetrical hydrogen bridge

(Table 2). On the other hand the NH resonance of the bisprotonated analogue [1+2H][PF₆, BF₄] (**3b**) is observed as a sharp singlet at δ = 7.84 (CD₃CN) as a consequence of the lack of N-H...N hydrogen bonding. In this context, it is noted that [1+2H][Cl, Cl₂H] (**3a**) gives a relatively sharp singlet at δ = 11.18, which is at lower field than [1+2H][PF₆, BF₄] (**3b**) because of hydrogen bonding to the chloride anion. Furthermore, there is a broad singlet in **3a** at δ = 4.33, which is assigned to the proton of the [Cl₂H]⁻ anion.^[35] The resonances in the aromatic region have a typical ABX pattern.

For the determination of the pK_{BH+} value,^[36, 37] UV/Vis spectroscopy could not be used because of the similarity of the spectra for both **1** and **2a**. Therefore, the basicity of **1** was determined by ¹H NMR measurements of transprotonation reactions.^[37–39] The sterically hindered guanidine MTBD proved to be the ideal base with sufficiently slow proton-exchange rates in the low-temperature ¹H NMR spectrum in CD₃CN. Other bases, such as DBU and PMG (Table 4), disclosed only coalesced signals as a result of fast proton-exchange processes. The experimental pK_{BH+} value of 25.1 ± 0.2^[40] for TMGN (**1**) was obtained by integration of the baseline-separated diagnostic resonances of the individual species **1** and **2a** (doublet at δ = 6.23 and 6.49, respectively). It is in excellent agreement with the theoretically calculated value for the absolute proton affinity (APA) in MeCN: 25.4.^[41] The comparison with tetramethylphenylguanidine (TMPhG, pK_{BH+} = 20.6, Table 4) states unquestionably that there is a cooperative effect of both chelating guanidine functions which overcompensates inductive effects of the naphthalene system. This value is almost in the range of monoiminophosphoranes, for example IPNMe (Table 4), and even considerably higher than most ordinary guanidines.^[18a, 19c, 42]

From the pK_{BH+} determination it became clear that, in contrast to classical proton sponges,^[15a,b, 23, 27] **1** allows rather

Table 4. Relative basicity values.

Base	pK _{BH+} (MeCN)
vinamidine (VA)	31.94 ^[17]
(Me ₂ N) ₂ P=NMe (IPNMe)	27.58 ^[19c, 62]
MTBD 	25.43 ^[18b, 19c]
TMGN (1)	25.1 ^[a]
(Me ₂ N) ₂ C=NMe (PMG)	25.00 ^[19c]
DBU	24.32 ^[19c]
(Me ₂ N) ₂ C=NH (TMG)	23.3 ^[19c]
(Me ₂ N) ₂ C=NPh (TMPhG)	20.6 ^[18a, 20a]
DMAN	18.18 ^[5, 63]
quinolino[7,8-h]quinoline (QQ)	12.8 ^[14b] (DMSO)

[a] Present work.

fast rates of proton exchange which are required for applications as auxiliary bases in base-catalyzed reactions. This will be demonstrated in particular by comparing the proton self-exchange rates between the free base (**1**) and the monoprotonated form (**2a**) relative to the DMAN/DMANH⁺ system^[43] as a criterion for its kinetic activity. Equimolar amounts of **1** and **2a** were dissolved in CD₃CN, and ¹H NMR spectra of the mixture were recorded at temperatures ranging from 344 to 225 K with a coalescence signal at 300 K (500 MHz). The free energy of proton self-exchange was determined to be 59.3 kJ mol⁻¹ from an Eyring plot that resulted from a lineshape analysis of the variable-temperature ¹H NMR spectra (Figure 4).^[44] However, no coalescence could be observed for DMAN/DMANH⁺, either in CD₃CN or [D₆]DMSO up to temperatures of 336 and 371 K, respectively.^[45] Therefore, it can be estimated that DMAN should exhibit a free energy of proton exchange of >72.6 kJ mol⁻¹ ([D₆]DMSO) which is in the range of the activation enthalpy estimated for the exchange of D⁺ in DMAN/DMANH⁺.^[46]

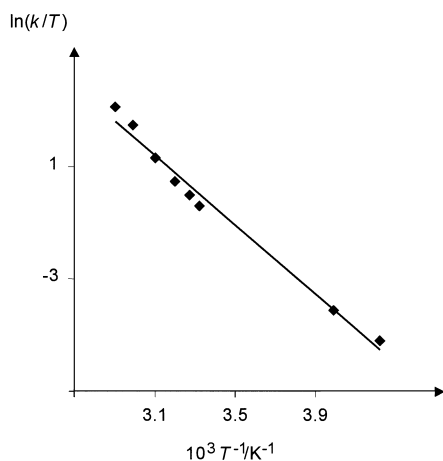


Figure 4. Eyring plot from proton self-exchange experiments of **1/2a**.

NMR spectra and molecular dynamics: The intrinsic dynamic behavior of the guanidine group, combined with the change in structure as a result of protonation, leads to complex intramolecular exchange processes which were investigated by dynamic ¹H NMR spectroscopy.

Free base 1: Compound **1** exhibits one signal for the methyl groups at room temperature. At lower temperatures, this signal splits into two signals of equal intensity (Figure 5), with a coalescence point at $T_c = 253$ K (400 MHz), which is attributed to hindered rotation about the C=N bond (Figure 6). This is caused by the typical *syn-anti* isomerization of guanidines, which is already documented in the literature for other guanidine^[24, 47, 48] and TMG^[49] systems.

Generally, this isomerization can be caused by rotation or inversion, but in the case of **1**, only the rotation has to be considered for steric reasons and inversion is unlikely. At ambient temperature, the protons of the two *N*-dimethylamino units are equivalent. Thus, a flip model^[50] with two separate ground-state conformers,^[7c] such as that observed in DMAN, where free rotation is impossible because of the repulsion

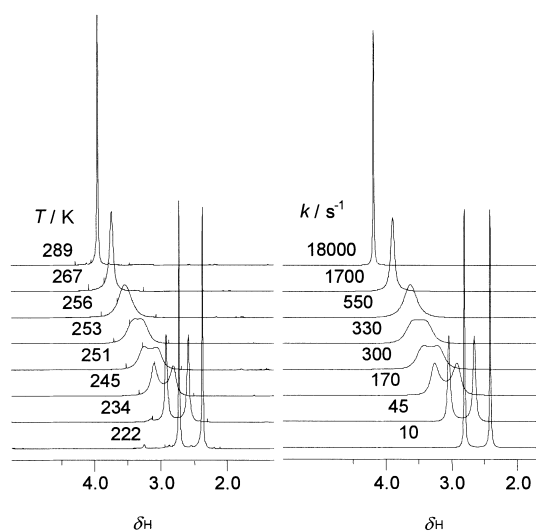


Figure 5. Temperature-dependent ¹H NMR spectra at 400 MHz for the *N*-methyl singlet of TMGN (**1**) in CD₂Cl₂ (experimental spectra: left, simulated by iterative fitting:^[49] right).

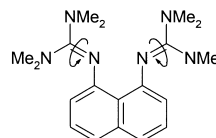


Figure 6. Rotation about the C=N double bond in TMGN (**1**).

between the methyl groups, cannot be present. Within the guanidine base **1**, the C–NR₂ single bonds rotate rapidly with respect to the NMR timescale, even at low temperatures.^[51]

From an Eyring plot, the free energy of activation ΔG^\ddagger for **1** was determined to be 49.0 kJ mol⁻¹ (256 K), which corresponds to 49.3 kJ mol⁻¹ at 238 K. This value is in agreement with the 50.7 kJ mol⁻¹ (at $T_c = 238$ K, 60 MHz) measured with TMPHG.^[49a] Of course, these values vary from alkyl-substituted guanidines, which exhibit a reasonably higher barrier of activation (PMG: $\Delta G^\ddagger = 78.7$ kJ mol⁻¹ at $T_c = 351$ K, 100 MHz^[48d]) because the C=N double bond is not weakened by inductive effects of the aromatic system. In **1**, however, a considerable weakening of the C=N bond order is realized by inductive effects of the naphthalene ring.

Monoprotonated 1: The low-temperature ¹H NMR spectrum of **2a** reveals four separate resonances (1:1:1:1) at 190 K (Figure 7) and is markedly more complicated than that of the free base **1**. It also differs significantly from the known spectra of [HTMPHG]⁺ and [PMPHG]⁺.^[47]

The fact that **2a** also exhibits real proton sponge properties in solution with a rapidly exchanging proton in an IHB (Scheme 3), is documented in the number of aromatic proton signals, along with the number of methyl signals in the range of fast exchange. Unsymmetrical protonation would result in six resonances in the aromatic region and two for the methyl signals. In **2a** only three aromatic signals and one methyl signal is observed, indicating the equivalence of both basic centers. Now two exchange phenomena are possible, leading to the four methyl resonances in the low-temperature spectrum. A single concerted process with all four of the

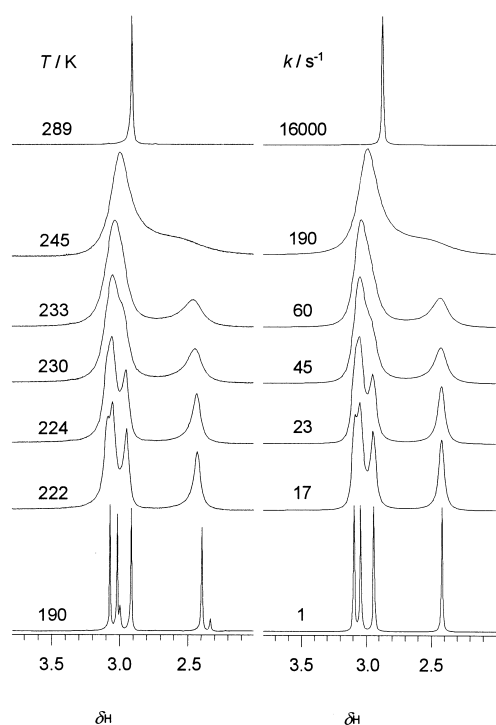
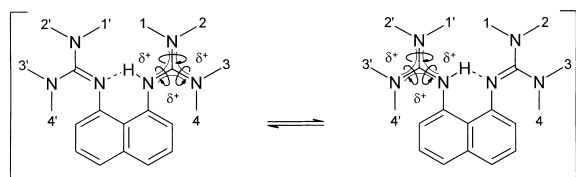


Figure 7. Temperature-dependent ^1H NMR spectra at 400 MHz for the *N*-methyl singlet of $[\mathbf{1}+\text{H}][\text{PF}_6]$ ($\mathbf{2a}$) in CD_2Cl_2 (experimental spectra: left, simulated by iterative fitting:^[49] right).

guanidine units exchanging at the same time. Otherwise, one rotation would be preferably restricted if the energy content of the partial double bonds would significantly differ from each other (probably as a result of conjugation of the former C=N double bond with the aromatic ring system). The latter should first cause a symmetrical split (1:1) into two singlets, followed by a second split of the two singlets at even lower temperatures into another set of singlets, which can be seen in part in $[\text{RTMPHG}]^+$ ($\text{R} = \text{H}, \text{Me}$).^[47]



Scheme 3. Rotation about partial C=N double bonds in $[\mathbf{1}+\text{H}][\text{PF}_6]$ ($\mathbf{2a}$) with equilibration of the proton.

There are several indications of a single concerted process in the variable-temperature spectra of $\mathbf{2a}$. In the ^1H NMR spectra of $\mathbf{2a}$ recorded below 249 K (T_c^1), firstly an unsymmetrical separation of the singlet for the *N*-methyl protons with an intensity of 3:1 becomes visible; this excludes a sequential process. Thereafter, the downfield signal gradually splits into three singlets (1:1:1) that exhibit a similar chemical shift which is significantly different from the signal at higher field (for studies on mesomeric cations, see ref. [52]). Moreover, the concerted process is confirmed by the free energies of activation of the three observable coalescence phenomena that are obtained from an Eyring plot and are very similar

with ΔG^\ddagger_1 (249 K) = 48.7, ΔG^\ddagger_2 (231 K) = 48.6, and ΔG^\ddagger_3 (224 K) = 48.5 kJ mol^{-1} (all recorded at 400 MHz). Furthermore, the lineshape analysis on the basis of a single concerted process as the exchange mechanism leads to an excellent agreement with the obtained experimental spectra. In addition, the ΔG^\ddagger values determined from the resulting Eyring plot are in good agreement with those received from the calculations based on the experimental coalescence points. They are in the range of the activation barriers found in $[\text{HTMPHG}]^+$ ^[47c] (ΔG^\ddagger_1 (248 K) = 52.3, ΔG^\ddagger_2 (248 K) = 54.0, and ΔG^\ddagger_3 (225 K) = 46.9 kJ mol^{-1} , all recorded at 60 MHz) and quite contradictory to $[\text{PMPHG}]^+$ ^[47a] (only ΔG^\ddagger_1 (301 K) = 64.9 and ΔG^\ddagger_2 (227 K) = 46.5 kJ mol^{-1} were determined at 60 MHz). These findings are in good agreement with the values of benzyl-substituted guanidinium salts which show considerably higher free energies of activation ($[\text{B}_2\text{TMG}]^+$: ΔG^\ddagger (at $T_c = 276$ K, 60 MHz) = 61.1 kJ mol^{-1} ^[48b]) since there is no weakening of the C=N bond by the adjacent aromatic system resulting in lower energy barriers. In summary, the described behavior is a convincing argument that a true IHB with a rapidly equilibrating proton is formed, both guanidine groups are indiscriminate within the observed temperature region (as is reported for the NMe_2 units of DMANH^+ ^[46]). It is assumed that $[\mathbf{1}+\text{H}][\text{PF}_6]$ ($\mathbf{2a}$) possesses a symmetrical double minimum energy profile with a low barrier of transition.^[5, 53]

Bisprotonated 1: On account of the insolubility of hydrochloride $\mathbf{3a}$ in CD_2Cl_2 at low temperatures, the triflate $\mathbf{3c}$ was employed for the kinetic NMR studies (Figure 8). The low-temperature ^1H NMR spectra of $[\mathbf{1}+2\text{H}][\text{OTf}]_2$ ($\mathbf{3c}$) resemble those of $[\mathbf{1}+\text{H}][\text{PF}_6]$ ($\mathbf{2a}$) down to a temperature of 222 K. The split of the methyl resonances follow the same interpretation, and it becomes clear that the proton exchange in the IHB of $\mathbf{1}+\text{HPF}_6$ ($\mathbf{2a}$) does not affect the splitting of the signal, otherwise the spectra of mono- and bisprotonated $\mathbf{1}$ should differ.

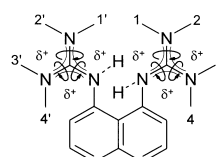


Figure 8. Rotation about partial C=N double bonds in $[\text{TMGNH}_2]^{2+}$.

The free energies of activation for the first three coalescences of $\mathbf{3c}$ (similar to $\mathbf{2a}$) are calculated from the coalescence points in the experimental spectra: $\Delta G_{T_c}^\ddagger = 48.2/47.3/45.4$ kJ mol^{-1} ($T_c = 256/235/226$ K). In the TMGN system and its protonated species, contrary steric and electronic effects seem to interfere. Taking only the electronic effect into account, the C=N bond order and barrier to rotation is expected to decrease with the extent of protonation. Whereas the ΔG^\ddagger values do not reflect this prediction, the ΔH^\ddagger values, although hampered with a large experimental error,^[54] are much better at demonstrating the expected trend of lowering the activation barriers of the base and its corresponding mono- and bisprotonated acids (Table 5).

Table 5. Free activation energies and enthalpies of rotation, *syn*–*anti* conformation and self-exchange in the bis(guanidine) proton sponge system.^[a]

Compound	$\Delta G_{298}^{\ddagger}$ [kJ mol ⁻¹] ^[64]	$\Delta G_{256}^{\ddagger}$ [kJ mol ⁻¹] ^[64]	ΔH^{\ddagger} [kJ mol ⁻¹] ^[64]
TMGN (1) ^[b]	48.3 ± 0.1	49.0 ± 0.1	53.4 ± 0.3
[TMGNH]PF ₆ (2a) ^[b]	49.2 ± 0.1	48.8 ± 0.1	46.5 ± 0.3
[TMGNH ₂][OTf] ₂ (3c) ^[c]	51.9 ± 1.0	48.2 ± 0.1 ^[d]	27.0 ± 3.0
[TMGNH ₂][OTf] ₂ (3c) ^[b]	47.1 ± 0.1	45.6 ± 0.1	36.1 ± 0.3
<i>syn/anti</i> -N–H TMGN/[TMGNH] ⁺ ^[b] self-exchange	59.3 ± 0.1	58.2 ± 0.1	51.6 ± 0.3

[a] Activation entropy is omitted because of the large error in its determination.^[65] [b] Calculated from graphical analysis of rate constants obtained from simulated spectra.^[66] [c] Values obtained by extrapolation on the basis of the three experimentally determined individual $\Delta G_{T_c}^{\ddagger}$ values.^[54] [d] Value obtained from coalescence point ($T_c = 256$ K) of the experimental spectrum.^[67]

Below 222 K further coalescence phenomena are observed, the exchange rates between the *syn*- and the *anti*-conformation become detectable. Finally, at 190 K (400 MHz) no less than seven resonances are recorded for the guanidine methyl groups with two additional signals for the NH protons (Figure 9).

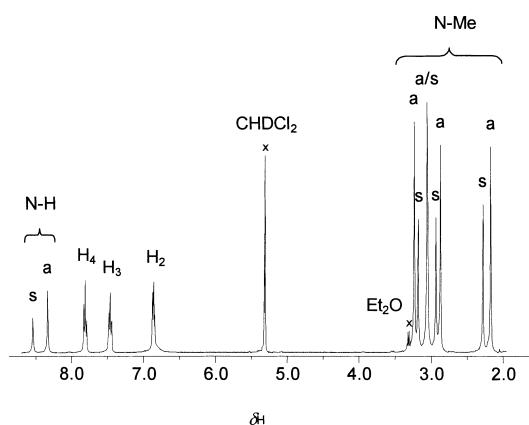


Figure 9. Low-temperature (190 K) ¹H NMR spectrum (400 MHz) of [1+2H][OTf]₂ in CD₂Cl₂.

Integration of the signals indicates a *syn/anti* population ratio of 42:58. In agreement with our preliminary crystal structure determination on **3b** and theoretical calculations on the gas-phase structure of bisprotonated **1**,^[41] it is assumed that the *anti* conformer is predominant in solution, especially if non-coordinating counteranions are employed. From the corresponding Eyring plot, the free energy of activation for the *syn*–*anti* equilibrium is calculated to be $\Delta G_{298}^{\ddagger} = 47.1$ kJ mol⁻¹ (Figure 10). It is interesting to note that in the bisprotonated **3c**, the $\Delta G_{298}^{\ddagger}$ value for the free energy of the *syn*–*anti* process (47.1 kJ mol⁻¹) is lower than the barrier to rotation (51.9 kJ mol⁻¹) about the C=N bonds.

Conclusion

TMGN (**1**) is a readily accessible and extremely basic guanidine derivative with the classical proton sponge back-

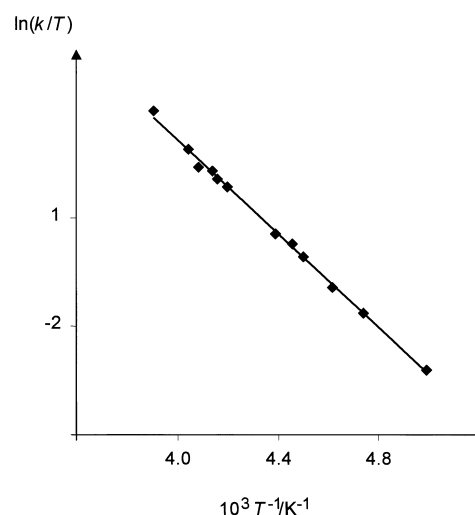


Figure 10. Graphical analysis of rate constants determined from spectra simulation for the *syn*–*anti* conformation equilibrium of [1+2H][OTf]₂ (**3c**).^[60]

bone of DMAN. To date it is the most basic compound in the class of naphthalene-based “proton sponges”. TMGN (**1**) has an experimentally determined pK_{BH^+} value of 25.1 ± 0.2 (MeCN) revealing a thermodynamic basicity nearly seven orders of magnitude higher than the parent DMAN. Furthermore, TMGN (**1**) also has a much higher kinetic basicity than DMAN, which is demonstrated by the kinetics of its proton self-exchange ($\Delta G_{298}^{\ddagger} = 59.3 \pm 0.1$ kJ mol⁻¹). On account of this high kinetic activity, the monoprotonated [1+H]⁺ may take up a second proton if treated with an excess of strong acid. TMGN is more stable to hydrolysis in comparison to the commercially available guanidine MTBD and less nucleophilic towards alkylating agents, such as C₂H₅I. Dynamic ¹H NMR studies on mono- and bisprotonated TMGN reveal a concerted mechanism of rotation about three almost equivalent C–N bonds. Furthermore, it is shown that there is an equilibrium between a *syn*- and an *anti*-conformation with respect to both guanidine functionalities of the bisprotonated **3c**. The base and corresponding acids are spectroscopically and structurally characterized. It is anticipated that a high thermodynamic basicity combined with a high kinetic activity is interesting for base-catalyzed applications.

Experimental Section

Materials and methods: All experiments were carried out in glassware assembled while hot in an inert atmosphere of argon 4.8 dried with P₄O₁₀ granulate. Solvents and triethylamine were purified according to literature procedures and also kept under an inert atmosphere. 1,8-Diaminonaphthalene (Merck) was purified by distillation from zinc dust.^[55] NH₄PF₆, NH₄ClO₄, trifluoromethanesulfonic acid (Aldrich), aqueous HPF₆ (60–65%, Strem Chemicals), HCl gas (MERCK), and ethyl iodide (Fluka) for protonation and alkylation, respectively, were used as purchased. Substances sensitive to moisture and air were kept in a nitrogen-flushed glove-box (Braun, Type MB 150 BG-I). Spectra were recorded on the following spectrometers: NMR: Bruker DRX 500, DRX 400 and AMX 300; IR: Bruker IFS 88 FT; UV/Vis: Hitachi U-3410; MS(EI, 70 eV): Varian MATCH-7a; MS(FD): Finnigan MAT 95 S; MS (ESI): Hewlett Packard HP 5989 B; elemental analysis: Heraeus CHN-Rapid; melting points: Büchi MPB-540 (uncorrected).

Lineshape analysis: The lineshape analysis of the variable-temperature ^1H NMR spectra were analyzed with the dynamic NMR simulation program WIN-DYNA.^[44] Errors are quoted as defined by Binsch and Kessler.^[65]

Caution! Phosgene is a severe toxic agent that can cause pulmonary embolism and in case of heavy exposition may be lethal. Use only in a well-ventilated fume hood.

Tetramethylchloroformamidinium chloride:^[25] Phosgene was passed through a solution of tetramethylurea (50 g) in toluene (200 mL) kept at 0 °C in a flask equipped with a reflux condenser cryostated to -30 °C for 2 h. Subsequently, the phosgene inlet was closed and the solution was allowed to warm to room temperature. The mixture was stirred for another 24 h, while the reflux condenser was maintained at -30 °C. The white precipitate was filtered off, washed three times with dry diethyl ether, and dried in vacuo. Yield: $\approx 95\%$.

1,8-Bis(1,1,3,3-tetramethylguanidino)naphthalene (1, TMGN): A solution of the Vilsmeier salt $[(\text{Me}_2\text{N})_2\text{CCl}]\text{Cl}$ (10.26 g, 60.0 mmol) in acetonitrile (30 mL) was added under cooling on an ice bath to a solution of 1,8-diaminonaphthalene (4.8 g, 30.0 mmol) and triethylamine (6.1 g, 8.5 mL, 60.0 mmol) in acetonitrile (50 mL). After the exothermic reaction was complete the mixture was refluxed for 3 h and a clear solution developed. Subsequently, NaOH (2.4 g, 60.0 mmol) in water (15 mL) was added under vigorous stirring in order to deprotonate the HNET_3Cl . After removal of the solvent as well as excess NEt_3 , the precipitate was washed three times with dry diethyl ether to remove unreacted amine, and was then dried in vacuo. TMGN (**1**) was obtained by complete deprotonation of the bis(hydrochloride) with 50 % KOH (50 mL) and extraction of the aqueous phase with MeCN (3 \times 50 mL). The combined filtrates were evaporated to dryness and taken up in warm hexane (100 mL). The solution was dried over MgSO_4 , stirred with activated charcoal to eliminate impurities, and filtered warm through Celite. Recrystallization from hexane and drying in vacuo gave **1** as weakly beige crystals (9.03 g, 25.5 mmol, 85 %). M.p. 123 °C; ^1H NMR (400.1 MHz, CD_3CN , 25 °C): $\delta = 7.19$ (d, $^3J(\text{H}_4, \text{H}_3) = 8.3$ Hz, 2H; $\text{H}_4, 5$), 7.13 (dd, $^3J(\text{H}_3, \text{H}_4) \approx ^3J(\text{H}_3, \text{H}_2) \approx 7.5$ Hz, 2H; $\text{H}_3, 6$), 6.23 (d, $^3J(\text{H}_2, \text{H}_3) = 6.8$ Hz, 2H; $\text{H}_2, 7$), 2.65 (s, 24H; CH_3); ^1H NMR (400.1 MHz, $[\text{D}_6]\text{DMSO}$, 25 °C): $\delta = 7.16$ –7.09 (m, 4H; H_3 – H_6), 6.16 (dd, $^3J(\text{H}_2, \text{H}_3) = 6.7$ Hz, $^4J(\text{H}_2, \text{H}_4) = 1.6$ Hz, 2H; $\text{H}_2, 7$), 2.62 (s, 24H; CH_3); ^1H NMR (400.1 MHz, CD_2Cl_2 , 28 °C): $\delta = 7.21$ (dd, $^3J(\text{H}_4, \text{H}_3) = 8.3$ Hz, $^4J(\text{H}_4, \text{H}_2) = 1.3$ Hz, 2H; $\text{H}_4, 5$), 7.15 (dd, $^3J(\text{H}_3, \text{H}_4) \approx ^3J(\text{H}_3, \text{H}_2) \approx 7.5$ Hz, 2H; $\text{H}_3, 6$), 6.27 (dd, $^3J(\text{H}_2, \text{H}_3) = 7.1$ Hz, $^4J(\text{H}_2, \text{H}_4) = 1.5$ Hz, 2H; $\text{H}_2, 7$), 2.66 (s, 24H; CH_3); ^1H NMR (400.1 MHz, CD_2Cl_2 , -73 °C): $\delta = 7.18$ (d, $^3J(\text{H}_4, \text{H}_3) = 8.0$ Hz, 2H; $\text{H}_4, 5$), 7.12 (dd, $^3J(\text{H}_3, \text{H}_4) \approx ^3J(\text{H}_3, \text{H}_2) \approx 7.5$ Hz, 2H; $\text{H}_3, 6$), 6.29 (d, $^3J(\text{H}_2, \text{H}_3) = 7.2$ Hz, 2H; $\text{H}_2, 7$), 2.71 (s, 12H; CH_3), 2.32 (s, 12H; CH_3); ^{13}C NMR (100.6 MHz, CD_3CN , 25 °C): $\delta = 155.0$ (CN_3), 150.7, 137.4, 126.1, 119.8, 115.7 (aromat. C), 39.4 (CH_3); ^{13}C NMR (100.6 MHz, $[\text{D}_6]\text{DMSO}$, 25 °C): $\delta = 154.0$ (CN_3), 150.1, 136.7, 125.9, 122.7, 119.6, 115.2 (aromat. C), 39.7 (CH_3); IR (KBr): $\tilde{\nu} = 3440$ w (br), 3002 w, 2937 m, 1630 vs, 1593 s, 1558 s, 1493 s, 1452 m, 1431 m, 1371 s, 1233 m, 1135 s, 985 m, 830 m, 760 cm^{-1} ; UV/Vis (MeCN, $c = 2 \times 10^{-5}$ mol L^{-1}): λ_{max} (ϵ) = 349.0 (15 600), 235.0 (46 000), 213 nm (36 300); MS (FD, MeCN): m/z (%): 354 [M^+]; MS (EI, 70 eV): m/z (%): 354.0 (86.5) [M^+], 310.0 (7.7) [$\text{M} - \text{NMe}_2$] $^+$, 253.0 (26.1) [$\text{M} - \text{C}(\text{NMe}_2)_2$] $^+$, 100.0 (55.9) [$\text{C}(\text{NMe}_2)_2$] $^+$, 85.0 (100) [$\text{C}_4\text{H}_9\text{N}_2$] $^+$; elemental analysis calcd (%) for $\text{C}_{20}\text{H}_{30}\text{N}_6$ (354.50): C 67.76, H 8.53, N 23.71; found: C 67.55, H 8.53, N 23.53.

1,8-Bis(1,1,3,3-tetramethylguanidinium)naphthalene hexafluorophosphate (2a, [1+H][PF₆]): The monoprotonated hexafluorophosphate salt was obtained by treatment of the free guanidine base **1** (354 mg, 1.00 mmol) with a solution of NH_4PF_6 (1 equiv, 160 mg, 0.98 mmol) dissolved in MeCN (15 mL) and stirring for 1 h at 50 °C. The solvent was evaporated and the solid was redissolved in MeCN. The solution was stirred over activated charcoal and passed through Celite. Removal of the solvent and crystallization from MeCN/ Et_2O gave **2a** as colorless crystals in almost quantitative yield (476 mg, 0.95 mmol, 97 %). M.p. 255 °C; ^1H NMR (400.1 MHz, CD_3CN , 25 °C): $\delta = 14.28$ (brs, 1H; NH), 7.40 (d, $^3J(\text{H}_4, \text{H}_3) = 8.3$ Hz, 2H; $\text{H}_4, 5$), 7.34 (dd, $^3J(\text{H}_3, \text{H}_4) \approx ^3J(\text{H}_3, \text{H}_2) \approx 7.9$ Hz, 2H; $\text{H}_3, 6$), 6.49 (d, $^3J(\text{H}_2, \text{H}_3) = 7.5$ Hz, 2H; $\text{H}_2, 7$), 2.87 (s, 24H; CH_3); ^{13}C NMR (100.6 MHz, CD_3CN , 25 °C): $\delta = 159.8$ (CN_3), 142.9, 136.9, 126.7, 122.0, 114.2 (aromat. C), 39.9 (CH_3); IR (KBr): $\tilde{\nu} = 3325$ m, 2922 m, 1646 vs, 1547 s, 1473 m, 1431 m, 1410 m, 1371 m, 1278 vs, 1247 vs, 1171 s, 1153 s, 1068 m, 1034 vs, 848 m, 766 m, 639 s, 573 m, 517 cm^{-1} ; UV/Vis (MeCN, $c = 2 \times 10^{-5}$ mol L^{-1}): λ_{max} (ϵ) = 348.0 (14 300), 233.3 nm (50 800); MS (FD, MeCN):

m/z (%): 355 [$(\text{1H}_2)^+$]; elemental analysis calcd (%) for $\text{C}_{20}\text{H}_{31}\text{N}_6\text{PF}_6$ (500.5): C 48.00, H 6.24, N 16.79; found: C 47.92, H 6.08, N 16.16.

1,8-Bis(1,1,3,3-tetramethylguanidinium)naphthalene perchlorate (2b, [1+H][ClO₄]): The monoprotonated perchlorate salt was obtained by stirring **1** (354 mg, 1 mmol) and NH_4ClO_4 (115 mg, 0.98 mmol) in MeCN (15 mL) for 1 h at 50 °C. After evaporation of the solvent, the solid material was redissolved in dry MeCN, stirred over activated charcoal and filtered through Celite. The volatiles were removed in vacuo and **2b** was crystallized from MeCN/ Et_2O (428 mg, 0.94 mmol, 96 %) as colorless crystals. M.p. 229 °C (decomp.); ^1H NMR (400.1 MHz, $[\text{D}_6]\text{DMSO}$, 25 °C): $\delta = 14.19$ (brs, 1H; NH), 7.41–7.33 (m, 4H; H_3 –6), 6.50 (dd, $^3J(\text{H}_2, \text{H}_3) = 7.1$ Hz, $^4J(\text{H}_2, \text{H}_4) = 1.0$ Hz, 2H; $\text{H}_2, 7$), 2.87 (s, 24H; CH_3); ^1H NMR (400.1 MHz, CD_2Cl_2 , 28 °C): $\delta = 14.76$ (brs, 1H; NH), 7.40 (dd, $^3J(\text{H}_4, \text{H}_3) = 8.3$ Hz, $^4J(\text{H}_4, \text{H}_2) = 1.1$ Hz, 2H; $\text{H}_4, 5$), 7.33 (dd, $^3J(\text{H}_3, \text{H}_4) \approx ^3J(\text{H}_3, \text{H}_2) \approx 7.8$ Hz, 2H; $\text{H}_3, 6$), 6.43 (dd, $^3J(\text{H}_2, \text{H}_3) = 7.4$ Hz, $^4J(\text{H}_2, \text{H}_4) = 1.2$ Hz, 2H; $\text{H}_2, 7$), 2.93 (s, 24H; CH_3); ^1H NMR (400.1 MHz, CD_2Cl_2 , -83 °C): $\delta = 14.63$ (brs, 1H; NH), 7.32 (dd, $^3J(\text{H}_4, \text{H}_3) = 8.2$ Hz, $^4J(\text{H}_4, \text{H}_2) = 1.0$ Hz, 2H; $\text{H}_4, 5$), 7.28 (dd, $^3J(\text{H}_3, \text{H}_4) \approx ^3J(\text{H}_3, \text{H}_2) \approx 7.6$ Hz, 2H; $\text{H}_3, 6$), 2.30 (dd, $^3J(\text{H}_2, \text{H}_3) = 7.2$ Hz, $^4J(\text{H}_2, \text{H}_4) = 1.0$ Hz, 2H; $\text{H}_2, 7$), 3.08 (s, 6H; CH_3), 3.03 (s, 6H; CH_3), 2.93 (s, 6H; CH_3), 2.40 (s, 6H; CH_3); ^{13}C NMR (100.6 MHz, $[\text{D}_6]\text{DMSO}$, 25 °C): $\delta = 158.5$ (CN_3), 142.0, 136.0, 126.1, 121.4, 117.6, 113.5 (aromat. C), 39.5 (CH_3); IR (KBr): $\tilde{\nu} = 2917$ m, 1617 m, 1559 s, 1467 m, 1405 s, 1371 m, 1352 m, 1235 w, 1163 m, 1088 s, 1015 w, 830 m, 769 m, 622 cm^{-1} ; UV/Vis (MeCN, $c = 2 \times 10^{-5}$ mol L^{-1}): λ_{max} (ϵ) = 348.2 (14 400), 306.7 (6800), 233.3 nm (50 500); MS (FD, MeCN): m/z (%): 355 [$(\text{1H}_2)^+$]; elemental analysis calcd (%) for $\text{C}_{20}\text{H}_{31}\text{N}_6\text{ClO}_4$ (455.0): C 52.80, H 6.87, N 18.47; found: C 52.53, H 6.88, N 17.83.

1,8-Bis(1,1,3,3-tetramethylguanidinium)naphthalene dichloride (3a, [1+2H][Cl, Cl₂H]): Gaseous HCl was bubbled into a solution of **1** (354 mg, 1 mmol) in CH_2Cl_2 (10 mL) for 5 minutes. The clear, light yellow solution was stirred for 1 h. The precipitate, which formed after adding Et_2O , was washed with dry diethyl ether. Crystallization from MeCN gave **3a** as colorless crystals (495 mg, 0.98 mmol, 98 %). The product analyzed as an adduct with 1 molecule HCl and 1 molecule CH_3CN . M.p. 233 °C; ^1H NMR (400.1 MHz, CD_3CN , 25 °C): $\delta = 11.20$ (s, 2H; NH), 7.92 (d, $^3J(\text{H}_4, \text{H}_3) = 8.1$ Hz, 2H; $\text{H}_4, 5$), 7.54 (dd, $^3J(\text{H}_3, \text{H}_4) \approx ^3J(\text{H}_3, \text{H}_2) \approx 7.9$ Hz, 2H; $\text{H}_3, 6$), 7.02 (d, $^3J(\text{H}_2, \text{H}_3) = 7.2$ Hz, 2H; $\text{H}_2, 7$), 4.33 (brs, 1H; Cl_2H), 2.94 (s, 24H; CH_3); ^{13}C NMR (100.6 MHz, CD_3CN , 25 °C): $\delta = 161.3$ (CN_3), 137.5, 133.8, 128.6, 127.1, 123.9, 123.1 (aromat. C), 41.0 (CH_3); IR (KBr): $\tilde{\nu} = 3417$ m, 3033 m, 2916 m, 1636 s, 1540 s, 1467 m, 1429 m, 1406 m, 1371 m, 1337 m, 1300 m, 1172 m, 1066 m, 1019 m, 796 m, 772 cm^{-1} ; UV/Vis (MeCN, $c = 2 \times 10^{-5}$ mol L^{-1}): λ_{max} (ϵ) = 346.7 (11 800), 232.8 nm (50 200); MS (FD, MeCN): m/z (%): 389 [$(\text{1H}_2\text{Cl})^+$], 354 [$(\text{1H}_2)^+$]; elemental analysis calcd (%) for $\text{C}_{20}\text{H}_{32}\text{N}_6\text{Cl}_2 \cdot \text{HCl} \cdot \text{CH}_3\text{CN}$ (427.4+36.5+41.1 (504.9)): C 52.33, H 7.19, N 19.42; found: C 53.14, H 7.12, N 18.98.

1,8-Bis(1,1,3,3-tetramethylguanidinium)naphthalene hexafluorophosphate-tetrafluoroborate (3b, [1+2H][PF₆, BF₄]): An impure, HBF₄-containing sample of aqueous hexafluorophosphoric acid (0.35 mL, 60–65 %) was added dropwise to **1** (354 mg, 1 mmol) in CH_2Cl_2 (10 mL). Within seconds, a white precipitate developed which was washed with dry diethyl ether and dried in vacuo. The precipitate was recrystallized from MeOH to yield (554 mg, 0.92 mmol, 92 %) **3b** as light brown crystals. M.p. 227 °C; ^1H NMR (400.1 MHz, CD_3CN , 25 °C): $\delta = 7.94$ (d, $^3J(\text{H}_4, \text{H}_3) = 8.3$ Hz, 2H; $\text{H}_4, 5$), 7.84 (s, 2H; NH), 7.58 (dd, $^3J(\text{H}_3, \text{H}_4) \approx ^3J(\text{H}_3, \text{H}_2) \approx 7.8$ Hz, 2H; $\text{H}_3, 6$), 7.04 (d, $^3J(\text{H}_2, \text{H}_3) = 7.3$ Hz, 2H; $\text{H}_2, 7$), 2.95 (s, 24H; CH_3); ^{13}C NMR (100.6 MHz, CD_3CN , 25 °C): $\delta = 160.6$ (CN_3), 137.2, 132.8, 128.6, 127.3, 123.1, 121.7 (aromat. C), 41.6 (CH_3); ^{19}F NMR (188.3 MHz, CD_3CN , 25 °C): $\delta = -70.9$ (d, $^2J(\text{F}, \text{P}) = 706.6$ Hz, PF_6), -149.6 (s, BF_4); ^{31}P NMR (162.0 MHz, CD_3CN , 25 °C): $\delta = -142.9$ (sept., $^1J(\text{P}, \text{F}) = 706.5$ Hz, PF_6); ^{11}B NMR (96.3 MHz, $[\text{D}_6]\text{DMSO}$, 25 °C): $\delta = -1.2$ (s, BF_4); IR (KBr): $\tilde{\nu} = 3383$ m, 2950 m, 1637 s, 1544 s, 1473 m, 1434 m, 1409 m, 1344 m, 1299 m, 1281 m, 1167 m, 1065 m, 1022 m, 841 s, 762 m, 558 cm^{-1} ; MS (ESI pos, MeCN): m/z (%): 501 [$(\text{1H}_2)\text{PF}_6^+$], 441 [$(\text{1H}_2)\text{BF}_4^+$], 355 [$(\text{1H}_2)^+$]; MS (ESI neg, MeCN): m/z (%): 145 [PF_6^-], 87 [BF_4^-]; elemental analysis calcd (%) for $\text{C}_{20}\text{H}_{32}\text{N}_6\text{BF}_{10}\text{P}$ (588.3): C 40.83, H 5.48, N 14.29; found: C 40.54, H 5.29, N 13.90.

1,8-Bis(1,1,3,3-tetramethylguanidinium)naphthalene bistriflate (3c, [1+2H][OTf]₂): Compound **1** (354 mg, 1 mmol) diluted in dry Et_2O (30 mL) was added dropwise to trifluoromethanesulfonic acid (0.9 mL, 10 mmol), which resulted in the instant precipitation of the bisprotonated triflate salt. Subsequently, the suspension was stirred for another 2 h, and

the precipitate was filtered and washed with dry Et₂O three times. Recrystallization from MeCN/Et₂O gave **3c** as colorless crystals (602 mg, 0.92 mmol, 92%). M.p. 242 °C; ¹H NMR (400.1 MHz, CD₃CN, 25 °C): δ = 8.08 (s, 2H; NH), 7.93 (d, ³J(H4,H3) = 8.3 Hz, 2H; H4,5), 7.57 (dd, ³J(H3,H4) ≈ ³J(H3,H2) ≈ 7.9 Hz, 2H; H3,6), 7.04 (d, ³J(H2,H3) = 7.5 Hz, 2H; H2,7), 2.95 (s, 24H; CH₃); ¹H NMR (400.1 MHz, CD₂Cl₂, 28 °C): δ = 8.51 (s, 2H; NH), 7.86 (d, ³J(H4,H3) = 7.7 Hz, 2H; H4,5), 7.52 (dd, ³J(H3,H4) ≈ ³J(H3,H2) ≈ 8.1 Hz, 2H; H3,6), 6.91 (d, ³J(H2,H3) = 7.5 Hz, 2H; H2,7), 2.96 (s, 24H; CH₃); ¹H NMR (400.1 MHz, CD₂Cl₂, –92 °C): δ = 8.54 (*syn* population 42% × 2H each NH), 8.34 (*anti* population 58% × 2H each NH), 7.87–7.75 (m, 2H; H4,5), 7.53–7.40 (m, 2H; H3,6), 6.93–6.75 (m, 2H; H2,7), 3.23, 3.05, 2.87, 2.17 (*anti* population 58% × 6H each CH₃), 3.18, 3.06, 2.94, 2.28 (*syn* population 42% × 6H each CH₃); ¹H NMR (400.1 MHz, CD₂Cl₂, 25 °C): δ = 8.51 (s, 2H; NH), 7.86 (d, ³J(H4,H3) = 7.7 Hz, 2H; H4,5), 7.52 (dd, ³J(H3,H4) ≈ ³J(H3,H2) ≈ 8.1 Hz, 2H; H3,6), 6.91 (d, ³J(H2,H3) = 7.5 Hz, 2H; H2,7), 2.96 (s, 24H; CH₃); ¹³C NMR (100.6 MHz, CD₃CN, 25 °C): δ = 160.7 (CN₃), 137.2, 133.0, 128.6, 127.2, 123.2 (aromat. C), 40.6 (CH₃); IR (KBr): $\tilde{\nu}$ = 3436 w (br), 2809 w, 1631 m, 1590 m, 1562 s, 1539 s, 1512 s, 1469 m, 1450 m, 1415 s, 1368 m, 1350 m, 1159 m, 1067 m, 1016 m, 837 vs, 767 m, 557 m cm⁻¹; MS (FD, MeCN): *m/z* (%): 505 [(1H₂)OTF]⁺, 355 [(1)H₂]⁺; elemental analysis calcd (%): for C₂₀H₃₂N₆F₆O₆S₂ (654.7): C 40.36, H 4.93, N 12.84; found: C 39.98, H 4.89, N 12.35.

¹H NMR self-exchange experiment: Equimolar amounts of TMGN (**1**) (1.81 mg, 5 × 10⁻⁶ mol) and [1+H][PF₆]⁻ (**2a**, 2.50 mg, 5 × 10⁻⁶ mol) were dissolved together in dry CD₃CN (0.5 mL), and ¹H NMR spectra were recorded at various temperatures ranging from 344 to 225 K. An analogous experiment was carried out with DMAN (4.28 mg, 2 × 10⁻⁵ mol) and DMANH⁺ (7.20 mg, 2 × 10⁻⁵ mol) in dry CD₃CN (0.9 mL) and dry [D₆]DMSO (0.8 mL), respectively.

¹H NMR basic hydrolysis experiment: TMGN (**1**, 21.3 mg, 6 × 10⁻⁵ mol) and MTBD (9.0 mg, 6 × 10⁻⁵ mol) were each dissolved in dry [D₆]DMSO (0.5 mL). After the addition of NaOD in D₂O (0.1 mL, 5 M) their ¹H NMR spectra were recorded at various times (*t* = 0 → 1 h/RT → 1 d/RT → 3 h/60 °C → 1 d/60 °C → 5 d/60 °C).

¹H NMR nucleophilicity experiment: TMGN (**1**, 46.3 mg, 1.3 × 10⁻⁴ mol) and MTBD (20.0 mg, 1.3 × 10⁻⁴ mol) were each dissolved in dry CD₂Cl₂ (0.6 mL) and C₂H₅I (TMGN: 102 mg, 0.053 mL, 6.5 × 10⁻⁴ mol; MTBD: 51 mg, 0.026 mL, 3.25 × 10⁻⁴ mol) was added, 2.5 equiv of the alkylating agent per guanidine function, respectively. The ¹H NMR spectra were recorded at various times (*t* = 0 → 15 min/RT → 1 h/RT → 1 d/RT → 3 d/RT).

X-ray structure analysis: Crystal data and experimental conditions are listed in Table 6. The molecular structures are illustrated as Schackal^[56] plots in Figures 1–4. Selected bond lengths and angles with standard deviations in parentheses are presented in Table 1. The collected reflections were corrected for Lorentz and polarization effects. All structures were solved by direct methods and refined by full-matrix least-squares methods on *F*².^[57] Hydrogen atoms were calculated and isotropically refined, except for H(1A) (**2a**) and H(1)/H(2)/H(4) (**3a**) which were found and isotropically refined.^[58] The correctness of the absolute structure of **2a** was confirmed by the Flack parameter refined to 0.01(5).

Acknowledgement

This work was supported by the DFG, SFB260, and by the Fonds der Chemischen Industrie. We would also like to thank Professor Z. B. Maksić, Zagreb, for stimulating discussions.

Table 6. Crystal data and structure refinement for **1**, **2a**, and **3a**.

Complex	TMGN (1)	[1+H][PF ₆] ⁻ (2a)	[1+2H][Cl, Cl ₂ H] (3a)
empirical formula	C ₂₀ H ₃₀ N ₆	C ₂₀ H ₃₁ N ₆ F ₆ P	C ₂₀ H ₃₂ N ₆ Cl ₂ × HCl, CH ₃ CN
<i>F</i> _w [g mol ⁻¹]	354.5	500.5	504.9
<i>T</i> [K]	183(2)	213(2)	213(2)
crystal system	monoclinic	monoclinic	monoclinic
space group	<i>P</i> 2 ₁ / <i>n</i>	<i>P</i> 2 ₁	<i>P</i> 2 ₁ / <i>c</i>
<i>a</i> [pm]	1313.7(1)	873.8(1)	1083.0(1)
<i>b</i> [pm]	1165.1(2)	1151.5(1)	3374.5(1)
<i>c</i> [pm]	1480.1(1)	1240.9(1)	743.5(1)
α [°]	90	90	90
β [°]	113.786(6)	107.003(5)	101.311(4)
γ [°]	90	90	90
<i>V</i> [Å ³]	2072.9(4)	1194.1(1)	2664.3(2)
<i>Z</i>	4	2	4
ρ [Mg m ⁻³]	1.136	1.392	1.259
μ [mm ⁻¹]	0.071	1.629	3.292
<i>F</i> (000)	768	524	1072
crystal size [mm ³]	0.50 × 0.30 × 0.30	0.40 × 0.40 × 0.20	0.45 × 0.27 × 0.12
diffractometer	Enraf Nonius CAD4	Enraf Nonius CAD4	Enraf Nonius CAD4
λ [pm]	Mo _{Kα} /71.073	Cu _{Kα} /154.178	Cu _{Kα} /154.178
scan technique	ω scan	ω scan	ω scan
θ range for data collection [°]	2.43–24.87	3.72–59.94	2.62–59.90
index ranges	–14 ≤ <i>h</i> ≤ 13 –13 ≤ <i>k</i> ≤ 0 0 ≤ <i>l</i> ≤ 17	–9 ≤ <i>h</i> ≤ 9 –12 ≤ <i>k</i> ≤ 0 0 ≤ <i>l</i> ≤ 13	0 ≤ <i>h</i> ≤ 12 0 ≤ <i>k</i> ≤ 37 –8 ≤ <i>l</i> ≤ 8
reflns collected	3725	1967	4166
independent reflns	3315	1875	3942
<i>R</i> _{int}	0.0354	0.0156	0.0478
obs. reflns [<i>F</i> ≥ 4σ(<i>F</i>)]	1970	1868	3468
data/restraints/parameters	3315/0/243	1875/0/307	3942/0/310
GoF on <i>F</i> ²	0.992	1.070	1.054
<i>R</i> ₁ [<i>F</i> ₀ ≥ 4σ(<i>F</i>)] ^[a]	0.0552	0.0627	0.0573
<i>wR</i> ₂ (all data) ^[a]	0.1575	0.1404	0.1681
transmission (max/min)	0.9791/0.9655	0.7365/0.5619	0.6934/0.3189
largest diff. peak and hole [e Å ⁻³]	0.147/–0.214	0.952/–0.754	0.676/–0.400

$$[a] R_1 = \sum |F_0| - |F_c| / \sum |F_0|; wR_2 = \{\sum [w(F_0^2 - F_c^2)^2] / \sum [w(F_0^2)^2]\}^{1/2}.$$

- [1] R. W. Alder, P. S. Bowman, W. R. S. Steele, D. R. Winterman, *J. Chem. Soc. Chem. Commun.* **1968**, 723–724.
- [2] R. W. Alder, *Chem. Rev.* **1989**, 89, 1215–1223.
- [3] H. A. Staab, T. Saupe, *Angew. Chem.* **1988**, *100*, 895–909; *Angew. Chem. Int. Ed. Engl.* **1988**, *27*, 865–879.
- [4] A. L. Llamas-Saiz, C. Foces-Foces, J. Elguero, *J. Mol. Struct.* **1994**, *328*, 297–323.
- [5] A. F. Pozharskii, *Russ. Chem. Rev.* **1998**, *67*, 1–24.
- [6] a) M. Pietrzak, J. Wehling, H.-H. Limbach, N. S. Golubev, C. López, R. M. Claramunt, J. Elguero, *J. Am. Chem. Soc.* **2001**, *123*, 4338–4339; b) H. A. Staab, A. Kirsch, T. Barth, C. Krieger, F. A. Neugebauer, *Eur. J. Org. Chem.* **2000**, 1617–1622; c) H. A. Staab, K. Elbl-Weiser, C. Krieger, *Eur. J. Org. Chem.* **2000**, 327–333; d) P. Hodgson, G. C. Lloyd-Jones, M. Murray, T. M. Peakman, R. L. Woodward, *Chem. Eur. J.* **2000**, *6*, 4451–4460; e) C. Cox, H. Wack, T. Lectka, *Angew. Chem.* **1999**, *111*, 864–867; *Angew. Chem. Int. Ed. Engl.* **1999**, *38*, 798–800; f) J. P. H. Charmant, G. C. Lloyd-Jones, T. M. Peakman, R. L. Woodward, *Eur. J. Org. Chem.* **1999**, 2501–2510; g) J. P. H. Charmant, G. C. Lloyd-Jones, T. M. Peakman, R. L. Woodward, *Tetrahedron Lett.* **1998**, *39*, 4733–4736; h) H. A. Staab, C. Krieger, G. Hieber, K. Oberdorf, *Angew. Chem.* **1997**, *109*, 1946–1949; *Angew. Chem. Int. Ed. Engl.* **1997**, *36*, 1884–1886.
- [7] a) S. T. Howard, *J. Am. Chem. Soc.* **2000**, *122*, 8238–8244; b) V. A. Ozeryanskii, A. F. Pozharskii, G. R. Milgizina, S. T. Howard, *J. Org. Chem.* **2000**, *65*, 7707–7709; c) P. R. Mallinson, K. Wozniak, C. C. Wilson, K. L. McCormack, D. S. Yufit, *J. Am. Chem. Soc.* **1999**, *121*, 4640–4646; d) S. T. Howard, J. A. Platts, *J. Org. Chem.* **1998**, *63*, 3568–3571; e) A. Szemik-Hojniak, J. M. Zwier, W. J. Buma, R. Bursi, J. H. van der Waals, *J. Am. Chem. Soc.* **1998**, *120*, 4840–4844; f) P. R. Mallinson, K. Wozniak, G. T. Smith, K. L. McCormack, *J. Am. Chem. Soc.* **1997**, *119*, 11502–11509; g) M. Peräkylä, *J. Org. Chem.* **1996**, *61*, 7420–7425; h) J. A. Platts, S. T. Howard, *J. Org. Chem.* **1996**, *61*, 4480–4482; i) A. L. Llamas-Saiz, C. Foces-Foces, A. Martínez, J. Elguero, *J. Chem. Soc. Perkin Trans. 2* **1995**, 923–927.
- [8] H. A. Staab, T. Saupe, C. Krieger, *Angew. Chem.* **1983**, *95*, 748–749; *Angew. Chem. Int. Ed. Engl.* **1983**, *22*, 731–732.
- [9] H. A. Staab, M. Höne, C. Krieger, *Tetrahedron Lett.* **1988**, *29*, 1905–1908.
- [10] T. Saupe, C. Krieger, H. A. Staab, *Angew. Chem.* **1986**, *98*, 460–461; *Angew. Chem. Int. Ed. Engl.* **1986**, *25*, 451–452.
- [11] H. A. Staab, M. Höne, C. Krieger, *Tetrahedron Lett.* **1988**, *29*, 5629–5632.
- [12] R. W. Alder, M. R. Bryce, N. C. Goode, N. Miller, J. Owen, *J. Chem. Soc. Perkin Trans. 1* **1981**, 2840–2847.
- [13] a) W. Wong-Ng, S. C. Nyburg, A. Awwal, R. Jankie, A. J. Kresge, *Acta Crystallogr. Sect. B* **1982**, *38*, 559–564; b) Y. Nagawa, M. Goto, K. Honda, H. Nakanishi, *Acta Crystallogr. Sect. C* **1986**, *42*, 478–480; c) G. Rimmler, C. Krieger, F. A. Neugebauer, *Chem. Ber.* **1992**, *125*, 723–728.
- [14] a) C. Krieger, I. Newsom, M. A. Zirnstein, H. A. Staab, *Angew. Chem.* **1989**, *101*, 72–73; *Angew. Chem. Int. Ed. Engl.* **1989**, *28*, 84–86; b) M. A. Zirnstein, H. A. Staab, *Angew. Chem.* **1987**, *99*, 460–461; *Angew. Chem. Int. Ed. Engl.* **1987**, *26*, 460–461; c) P. G. Jones, *Z. Kristallogr.* **1993**, *208*, 341–343.
- [15] a) R. W. Alder, N. C. Goode, N. Miller, F. Hibbert, K. P. P. Hunte, H. J. Robbins, *J. Chem. Soc. Chem. Commun.* **1978**, 89–90; b) F. Hibbert, K. P. P. Hunte, *J. Chem. Soc. Perkin Trans. 2* **1983**, 1895–1899; c) F. Hibbert, G. R. Simpson, *J. Chem. Soc. Perkin Trans. 2* **1987**, 243–246.
- [16] a) H. A. Staab, M. Diehm, C. Krieger, *Tetrahedron Lett.* **1994**, *35*, 8357–8360; b) H. A. Staab, M. A. Zirnstein, C. Krieger, *Angew. Chem.* **1989**, *101*, 73–75; *Angew. Chem. Int. Ed. Engl.* **1989**, *28*, 86–88.
- [17] R. Schwesinger, M. Mißfeld, K. Peters, H. G. von Schnering, *Angew. Chem.* **1987**, *99*, 1210–1212; *Angew. Chem. Int. Ed. Engl.* **1987**, *26*, 1165–1167.
- [18] a) I. Kaljurand, T. Rodima, I. Leito, I. A. Koppel, R. Schwesinger, *J. Org. Chem.* **2000**, *65*, 6202–6208; b) R. Schwesinger, *Chimia* **1985**, *39*, 269–272; c) G. Wieland, G. Simchen, *Liebigs Ann. Chem.* **1985**, 2178–2193; d) D. H. R. Barton, J. D. Elliot, S. D. Géro, *J. Chem. Soc. Perkin Trans. 1* **1982**, 2085–2090; e) D. H. R. Barton, J. K. Kervagoret, S. Z. Zard, *Tetrahedron Lett.* **1990**, *46*, 7587–7598.
- [19] a) P. A. S. Smith in *The Chemistry of Open-Chain Organic Nitrogen Compounds*, Vol. 1, W. A. Benjamin Inc., New York, **1965**, pp. 277–290; b) Y. Yamamoto, S. Kojima in *The Chemistry of Amidines and Imidates*, Vol. 2, Wiley, Chichester, **1991**, pp. 485–526; c) R. Schwesinger, *Nachr. Chem. Tech. Lab.* **1990**, *38*, 1214–1226.
- [20] a) K. T. Leffek, P. Pruszyński, K. Thanapaalasingham, *Can. J. Chem.* **1989**, *67*, 590–595; b) P. Pruszyński, *Can. J. Chem.* **1987**, *65*, 626–629.
- [21] P. Pruszyński, K. T. Leffek, B. Borecka, T. S. Cameron, *Acta Crystallogr. Sect. C* **1992**, *48*, 1638–1641.
- [22] a) W. Galezowski, M. Stanczyk, I. Grzeskowiak, A. Jarczewski, *J. Chem. Soc. Perkin Trans. 2* **1996**, 2647–2651; b) P. Pruszyński, K. T. Leffek, *Can. J. Chem.* **1991**, *69*, 205–210.
- [23] a) F. Hibbert, *Acc. Chem. Res.* **1984**, *17*, 115–120; b) F. Hibbert, *J. Chem. Soc. Perkin Trans. 2* **1974**, 1862–1866.
- [24] a) H. Wittmann, A. Schorm, J. Sundermeyer, *Z. Anorg. Allg. Chem.* **2000**, *626*, 1583–1590; b) H. Wittmann, V. Raab, A. Schorm, J. Plackmeyer, J. Sundermeyer, *Eur. J. Inorg. Chem.* **2001**, 1937–1948; c) V. Raab, J. Kipke, O. Burghaus, J. Sundermeyer, *Inorg. Chem.* **2001**, *40*, 6964–6971; d) V. Raab, J. Kipke, A. Schorm, J. Sundermeyer, unpublished results.
- [25] I. A. Cliffe in *Comprehensive Organic Functional Group Transformations*, Vol. 6, Elsevier, Oxford, **1987**, pp. 639–675.
- [26] a) B. Brzezinski, G. Schroeder, E. Grech, Z. Malarski, L. Sobczyk, *J. Mol. Struct.* **1992**, *274*, 75–81; b) J. Klimkiewicz, L. Stefaniak, B. Brzezinski, E. Grech, S. Kuroki, I. Ando, G. A. Webb, *J. Mol. Struct.* **1994**, *323*, 193–195.
- [27] R. W. Alder, M. R. Bryce, N. C. Goode, *J. Chem. Soc. Perkin Trans. 2* **1982**, 477–483.
- [28] A. Gobbi, G. Frenking, *J. Am. Chem. Soc.* **1993**, *115*, 2362–2372.
- [29] H. Einspahr, J. B. Robert, R. E. Marsh, J. D. Roberts, *Acta Crystallogr. Sect. B* **1973**, *29*, 1611–1617.
- [30] a) M. R. Truter, B. L. Vickery, *J. Chem. Soc. Dalton Trans.* **1972**, 395–402; b) K. Wozniak, T. M. Krygowski, B. Kariuki, W. Jones, E. Grech, *J. Mol. Struct.* **1990**, *240*, 111–118; c) J. A. Kanters, A. Schouten, J. Kroon, E. Grech, *Acta Crystallogr. Sect. C* **1991**, *47*, 807–810.
- [31] K. Wozniak, C. C. Wilson, K. S. Knight, W. Jones, E. Grech, *Acta Crystallogr. Sect. B* **1996**, *52*, 691–696.
- [32] E. Haselbach, A. Henriksson, F. Jachimowicz, J. Wirz, *Helv. Chim. Acta* **1972**, *55*, 1757–1759.
- [33] J. L. Atwood, S. G. Bott, C. M. Means, A. W. Coleman, H. Zhang, M. T. May, *Inorg. Chem.* **1990**, *29*, 467–470.
- [34] G. Y. S. Chan, M. G. B. Drew, M. J. Hudson, N. S. Isaacs, P. Byers, C. Madic, *Polyhedron* **1996**, *15*, 3385–3398.
- [35] According to a search of the CCDC database (May 2001), no NMR spectroscopic data are available in original publications of structurally characterized compounds with the $[\text{Cl}_2\text{H}]^-$ anion.
- [36] a) A. Albert, E. P. Serjeant in *The Determination of Ionization Constants*, Chapman & Hall, London, **1984**; b) C. H. Rochester in *Acidity Functions*, Vol. 17, Academic Press, London, **1970**, Chapt. 1.
- [37] R. F. Cookson, *Chem. Rev.* **1974**, *74*, 5–28.
- [38] a) F. Hibbert, *J. Chem. Soc. Chem. Commun.* **1973**, 463; b) A. Awwal, F. Hibbert, *J. Chem. Soc. Perkin Trans. 2* **1977**, 1589–1592; c) R. W. Alder, N. C. Goode, N. Miller, F. Hibbert, K. P. P. Hunte, H. J. Robbins, *J. Chem. Soc. Chem. Commun.* **1978**, 89–90; d) F. Hibbert, H. J. Robbins, *J. Am. Chem. Soc.* **1978**, *100*, 8239–8244; e) W. M. Latimer, W. H. Rodebush, *J. Am. Chem. Soc.* **1920**, *42*, 1419–1433.
- [39] T. Saupe, *Dissertation*, University of Heidelberg (Germany), **1985**.
- [40] Experimental error estimated from integration of ^1H NMR resonances ($\pm 2\%$) and weight content of **1** and MTBD in sample (± 0.01 mg).
- [41] See following paper, B. Kovačević, Z. B. Maksić, *Chem. Eur. J.* **2002**, *8*, 1694–1702. For recent publications on the APA of polyguanidines and other highly basic organic molecules, see: a) Z. B. Maksić, B. Kovačević, *J. Org. Chem.* **2000**, *65*, 3303–3309; b) Z. B. Maksić, B. Kovačević, *J. Phys. Chem. A* **1999**, *103*, 6678–6684; c) Z. B. Maksić, B. Kovačević, *J. Phys. Chem. A* **1998**, *102*, 7324–7328.
- [42] E. D. Raczynska, P.-C. Maria, J.-F. Gal, M. Decouzon, *J. Phys. Org. Chem.* **1994**, *7*, 725–733.
- [43] Synthesized analogous to **1**+HPF₆ (**2a**).
- [44] T. Lenzen, G. Hägele and Bruker Analytik GmbH, WIN-DYNA 32, Program for the Simulation and Iteration of Dynamic NMR, Heinrich-Heine University, Düsseldorf (Germany), **1994–1998**.
- [45] Maximum recording temperature; higher temperatures resulted in an inhomogeneous field (b.p. CD₃CN: 81 °C; [D₆]DMSO: 189 °C).
- [46] R. L. de Groot, D. J. Sikkema, *J. R. Neth. Chem. Soc.* **1976**, *95*, 10–14.

- [47] a) H. Kessler, D. Leibfritz, *Chem. Ber.* **1971**, *104*, 2158–2169; b) H. Kessler, *Angew. Chem.* **1970**, *82*, 237–253; *Angew. Chem. Int. Ed. Engl.* **1970**, *9*, 219–235; c) H. Kessler, D. Leibfritz, *Tetrahedron* **1969**, *25*, 5127–5145.
- [48] a) K. Kanamori, J. D. Roberts, *J. Am. Chem. Soc.* **1983**, *105*, 4698–4701; b) A. V. Santoro, G. Mickevicius, *J. Org. Chem.* **1979**, *44*, 117–120; c) H. Kessler, D. Leibfritz, *Tetrahedron Lett.* **1969**, *6*, 427–430; d) V. J. Bauer, W. Fulmor, G. O. Morton, S. R. Safir, *J. Am. Chem. Soc.* **1968**, *90*, 6846–6847.
- [49] a) H. Kessler, D. Leibfritz, *Tetrahedron* **1970**, *26*, 1805–1820; b) H. Kessler, D. Leibfritz, *Liebigs Ann. Chem.* **1970**, *737*, 53–60.
- [50] R. W. Alder, J. E. Anderson, *J. Chem. Soc. Perkin Trans. 2* **1973**, 2086–2088.
- [51] Minimum ¹H NMR recording temperature in CD₂Cl₂: 181 K.
- [52] a) H. O. Kalinowski, H. Kessler, *Org. Magn. Reson.* **1975**, *7*, 128–135; b) H. O. Kalinowski, H. Kessler, *Org. Magn. Reson.* **1974**, *6*, 305–312.
- [53] a) L. J. Altman, D. Laungani, G. Gunnarsson, H. Wennerström, S. Forsén, *J. Am. Chem. Soc.* **1978**, *100*, 8264–8266; b) G. Gunnarsson, H. Wennerström, W. Egan, S. Forsén, *Chem. Phys. Lett.* **1976**, *38*, 96–99.
- [54] ΔH^\ddagger and ΔG_{298}^\ddagger of [1+2H][OTf]₂ (**3c**) were obtained by extrapolation on the basis of the three experimentally determined individual $\Delta G_{T_c}^\ddagger$ values ($T_c = 256/235/226$ K).
- [55] H. O. House, D. G. Koepsell, W. J. Campbell, *J. Org. Chem.* **1972**, *37*, 1003–1011.
- [56] E. Keller, *Schakal-97*, Program for the Graphic Representation of Molecule and Crystallographic Models, **1997**, University of Freiburg (Germany).
- [57] a) G. M. Sheldrick, *SHELXS-97*, Program for Crystal Structure Solution and SHELXL-97, Program for Crystal Structure Refinement, University of Göttingen (Germany), **1997**; b) Siemens Analytical X-ray Instruments Inc., *SHELXTL 5.06*, Madison, WI (USA), **1995**.
- [58] CCDC-170726 (**1**), CCDC-170727 (**2a**) and CCDC-170728 (**3a**) contain the supplementary crystallographic data for this paper. These data can be obtained free of charge via www.ccdc.cam.ac.uk/conts/retrieving.html (or from the Cambridge Crystallographic Data Centre, 12 Union Road, Cambridge CB2 1EZ, UK; fax: (+44) 1223-336-033; or deposit@ccdc.cam.ac.uk).
- [59] T. Barth, C. Krieger, F. A. Neugebauer, H. A. Staab, *Angew. Chem.* **1991**, *103*, 1006–1008; *Angew. Chem. Int. Ed. Engl.* **1991**, *30*, 1028–1030.
- [60] U. Müller, H.-D. Dörner, *Z. Naturforsch. (B)* **1982**, *37*, 198–200.
- [61] A. Deeg, T. Dahlems, D. Mootz, *Z. Kristallogr. New Cryst. Struct.* **1997**, *212*, 401–402.
- [62] R. Schwesinger, H. Schlemper, *Angew. Chem.* **1987**, *99*, 1212–1214; *Angew. Chem. Int. Ed. Engl.* **1987**, *26*, 1167–1169.
- [63] pK_{BH^+} (MeCN, 22 °C): 18.50 according to A. F. Pozharskii, N. L. Chikina, N. V. Vistorobskii, V. A. Ozeryanskii, *Russ. J. Org. Chem.* **1997**, *33*, 1810–1813.
- [64] Experimental errors: $\Delta\nu = \pm 2$ Hz, $\Delta T = \pm 2$ K, and $\Delta k = \pm 2\%$ result in an error of $\Delta G^\ddagger/\Delta H^\ddagger = \pm 0.1/0.3$ kJ mol⁻¹.
- [65] G. Binsch, H. Kessler, *Angew. Chem.* **1980**, *92*, 445–463; *Angew. Chem. Int. Ed. Engl.* **1980**, *19*, 411–429.
- [66] Equations used: $\ln(k/T) = 23.76 - (\Delta H^\ddagger/R) \times 1/T + (\Delta S^\ddagger/R)$, $\Delta G^\ddagger = \Delta H^\ddagger - T\Delta S^\ddagger$; H. Günther in *NMR-Spektroskopie*, 3rd ed., Thieme, Stuttgart, New York, **1992**.
- [67] Calculated with: $\Delta G^\ddagger = 19.1 \times 10^{-3} \times T_c (9.97 + \log T_c - \log |\nu_A - \nu_B|)$; M. Hesse, H. Meier, B. Zeeh in *Spektroskopische Methoden in der organischen Chemie*, 4th ed., Thieme, Stuttgart, New York, **1991**.

Received: September 18, 2001 [F3560]